Feasibility study of an off-grid container unit for industrial construction

A.B. Kristiansen[a], D. Satola[b], K. Lee[c], B. Zhao[a], T. Ma[a], R.Z. Wang[a, *], A. Gustavsen[b], V. Novakovic[c]

[a] Institute of Refrigeration and Cryogenics, MOE Engineering Research center of Solar Energy, Shanghai Jiao Tong University, Shanghai 200240, China

[b] Norwegian University of Science and Technology, Department for Architectural Design, History and Technology. Research Centre of Zero Emission Neighbourhoods in Smart cities (FME-ZEN).

[c] Norwegian University of Science and Technology, Department of Energy and Process Engineering

* corresponding author: rzwang@sjtu.edu.cn

Abstract

This article presents solutions for improved energy efficiency by adapting a shipping container building in Shanghai for off-grid operation. While this prototype is based on a single unit, larger buildings made from multiple units constructed at factories is the ultimate goal. Previous studies of container buildings have revealed gaps concerning the quality of construction and thermal comfort. In this study, the heat transfer resistance of a typical container building wall has been improved from 1.0 m^2K/W to around 3.7 m^2K/W by installing Vacuum Insulation Panels (VIP), verified through measurements. VIPs reduce the temperature dependence of the heating need and the thermal bridges from the steel beams. Through validated building performance simulation using the software IDA ICE, the energy use and indoor air quality were examined for different ventilation scenarios and indoor temperature setpoints in Shanghai. A wider range of heating and cooling setpoints outside operation hours, lowering the heating setpoint at night and upgrading to

triple glazed windows were found to be the most economic energy saving measures. Combined with roof rainwater harvesting, the possibility of achieving near self-sufficiency of water and electricity in the suburbs of Shanghai shows promise in the quest for a higher degree sustainable living.

Keywords: Container building, off-grid, energy efficiency, ventilation, vacuum insulation panels, indoor air quality.

Highlights:

- Vacuum Insulation Panels reduced the heat load of a container unit in winter by 40%
- Upgrading to 3-layer glazed windows or reducing the window area is recommended
- Natural ventilation uses 7% more energy than forced ventilation with heat recovery
- Relaxed cooling and heating setpoints outside operation provide over 40% savings
- An increase of electricity and water self-sufficiency points to a sustainable future

Abbreviations

ACH50	Air Changes per Hour at 50 Pa pressure difference
AIVC	The Air Infiltration and Ventilation Centre (AIVC) is the International Energy Agency's information centre on energy efficient ventilation of buildings.

CLO	The clothing insulation in clo, where 1 clo equals 0.155 m^2K/W [1]
DHW	Domestic Hot Water
EE	Embodied Energy
g	Solar Heat Gain Coefficient (commonly referred to as SHGC)
GHG	Greenhouse Gas
HFM	Heat Flow Meter
HV	Hybrid Ventilation
HVAC	Heating, Ventilation and Air Conditioning
IEA	The International Energy Agency
IWEC	International Weather for Energy Calculation (database)
LCA	Life Cycle Assessment
MBE	Mean Bias Error
MET	Metabolic rate in metabolic units where 1 met equals 58 W/m^2 [1]
MV	Mechanical Ventilation
NPV	Net Present Value
NV	Natural Ventilation
NZEB	Net Zero Energy Building

PM2.5	Particulate Matter with a diameter of less than 2.5 micrometers
PCM	Phase Change Material
ppm	Parts per million
PV	Photovoltaics
RMSE	Root Mean Square Error
SEER	Seasonal Energy Efficiency Ratio defined according to the European Union standards EN14511 and EN14825 as described in chapter 2.4.1.2 in [2], corresponding to China's domestic standard GB21455.
SFP	Specific Fan Power
SCOP	Seasonal Coefficient of Performance, defined according to the European Union standards EN14511 and EN14825 as described in chapter 2.4.1.2 in [2], corresponding to China's domestic standard GB21455.
VIP	Vacuum Insulation Panel
ZEB	Zero Energy Building

1. Introduction

It is predicted that 60% of the world's population will live in cities by 2030, increasing to 70% by 2050 [3]. Worldwide, a 30 % increase in energy need for buildings is expected by 2040 [4]. A recent review by Kristiansen, et al. [5], which this article builds on, reveals how Photovoltaics (PV)

powered shipping container homes can provide affordable and decent zero energy homes with a 5-10 % reduction in material use. Compared to on-site construction it is also more sustainable because fewer leftover materials are left on site, more waste is recycled, transport to site is minimized and there are fewer accidents [3]. Moreover, numerous studies claim that modular construction reduces the construction time by 50-60% [3].

As China is projected to build a lot of substantial infrastructure works in the coming years through 'Belt-and-Road' initiatives, there is a need for transportable, decent, temporary housing. Constructing modular container modules that can be rearranged and upgraded and become permanent houses has become a viable alternative [6]? Governments should see these as potential cities of tomorrow. In the suburbs of cities there is enough land to build single-story homes, which benefit from the space for PV on the roof.

A container home is selected for this case study, in which the steel provides fire resistance, longevity and high load-bearing capacity which allows large spacing between the columns [3] [7]. Steel structures can be as sustainable as wood, as long as the structural steel is reused [7, 8]. A container-based structure makes it easier to transport the building back to the factory for reuse and recycling at the end of its lifetime. A literature review by McConnell and Bertolin [9] indicates that shipping containers are significantly cheaper than other prefabrication alternatives, and that they have high heat resistance with simple modifications. Still, the operational energy requirements is dominant topic in most studies of container buildings [7, 9], although Tumminia, et al. [10] demonstrated that for a Net Zero Energy Building the material production dominates. Design solutions based on the reuse and recycling of buildings tend to win proposals because they reduce costs and environmental impact [11].

Based on the presentation of ZEB definitions in the review by Kristiansen, et al. [5] it was chosen to focus on ZEB rather than Net ZEB or near ZEB, since this definition is easier for the public to understand and assures that the goal is to rely fully on solar energy in operation. Recently, off-grid container buildings have also been suggested more frequently lately [11-14], due to the potential of self-sufficiency. Although grid connection would be more economical in most cities, off-grid solutions are welcomed because they strengthen the focus on energy efficiency and motivates users to pay more attention to their energy use. The majority of the zero energy research projects have been located in Europe or the USA, where most researchers have focused on grid-connected net zero energy buildings that are built on site [15-18]. There is, therefore, a need for studies on factory-made, off-grid zero energy buildings.

Shanghai is suitable as the location of a container home factory since Shanghai is the busiest harbor in the world [19]. Furthermore, 90% of the world's shipping containers are produced in China [20]. The Chinese government strongly promotes building prefabricated buildings and has mandated that 15% of the nation's annual new construction be built in a prefabricated manner by 2020 and 30% by 2025 [21, 22]. Certainly, prices for such buildings will fall as production increases. For example, Irulegi, et al. [23] demonstrated that the unit cost was reduced by almost 30% by increasing the production from 18 units to 489 units.

1.1 Water harvesting

While the global population has increased by 300% during the 20th century, water demand has increased twice as fast [24]. In India, several states have consequently made it mandatory to install rainwater harvesting systems on the roofs of new buildings in urban areas [25]. The payback period for such systems is typically 2–6 years [26].

For arid regions, vapor compression condensing or an adsorption process can be used to extract water from the air. Atmospheric water-harvesting has seen clear progress during the last two decades [27]. It is now considered a reasonable way to obtain water in arid or desert areas [28]. A review of atmospheric water harvesting by Tu, et al. [27] points out that tank delivery or bottled water is expensive, while desalination depends on high operation and low maintenance costs to be viable for small scale applications. Through co-operation with solar energy, atmospheric water harvesting can provide a more sustainable solution. The optimal commercially available solution has an electricity use of around 250 Wh/kg. During periods with excess PV generation, this energy may be used to extract water from the air.

1.2 State of the art and research gaps

In the existing studies of buildings made from shipping containers and similar modular steel structures, control of heat gain through the windows and natural ventilation are often mentioned [10, 23, 29-33]. An overview of studies related to container buildings is included in Table A.1. On the other hand, research has shown that hybrid ventilation can result in considerable energy conservation in warm and humid climates, in comparison to natural ventilation and mechanical ventilation for stand-alone systems [34, 35]. There appears to be no studies that focus on ventilation scenario assessment in container buildings. Therefore, it is necessary to clarify the interrelations between ventilation scenario, energy demand, peak loads, and indoor air quality in container buildings.

A recent study of a container home for the hot and humid climate in Port Said showed a problem with thermal comfort. Five different models with different 100 mm insulation layers all showed around 4000-5000 discomfort hours per year [36]. Another study of a container building in a hot and humid tropical climate in India showed that the thermal indoor climate performance was as

good as a traditional building with brick walls and cement mortar. However, this can largely be attributed to the attached cement shading roof with an overhang [37]. Consequently, it is not directly comparable. It is also not transportable and has higher embodied GHG emissions because of the concrete.

One reason for the thermal discomfort is often the high infiltration of outdoor air. The airtightness of four container buildings commonly used for temporary housing in Turkey was measured in a study, with Air Changes per Hour at 50 Pa pressure difference (ACH50) between 9-25 h^{-1} [38]. An airtight building would have a leakage number in the range of 0.6-2 h^{-1} for ACH50, which indicates the need to increase the quality of container sealings.

There is also a gap in the quality of construction. A container wall is more challenging to insulate than an ordinary wall. Foam insulation can be used to level the surface and create a seamless moisture barrier to prevent corrosion, but it is more expensive than ordinary insulation methods [39]. If mineral wool is placed outside the foam insulation, an ordinary moisture barrier would not only reduce the diffusion of moisture from the room into the mineral wool, but also make the drying process very slow. A smart moisture barrier is probably the best solution, since it allows the wall to dry towards the inside during periods with low indoor humidity. The diffusion rate for a smart moisture barrier depends on the relative humidity on each side of the moisture barrier. During the winter, the relative humidity inside the building is higher than inside the external wall and the smart moisture barrier works like an ordinary moisture barrier [40, 41].

Various studies have tried to map energy efficiency in buildings [42-46], based on surveys performed in a variety of provinces in China. Out of the surveyed homes, 80 % had energy inefficient, single-pane windows [42, 44]. As for the wall construction layers, brick walls with a

U-value of 1W/m^{2}K were typically used [46]. For cooking purposes, about 49% of the surveyed households from the study of Wu, et al. [42] used a firewood-based stove, while the rest used gas-based (22%) and electric stoves (19%). Poor indoor air quality is caused by the use of inefficient stoves and insufficient ventilation [47]. Based on measurements of indoor PM2.5 and CO_2 concentration, improvements in indoor air quality is found to be critical [48].

To improve the thermal resistance of the envelope, Vacuum Insulation Panels (VIP) is considered. VIPs (3-8 mW/(mK)) have 5-10 times lower thermal conductivity compared to mineral wool, which makes it possible to achieve high thermal resistance without considerably reducing the already limited width of the container [49]. The design approach also involves a tiny and well-insulated space, similar to refrigerators, where VIPs are more commonly used. Because the area is small, the additional cost of using a more expensive insulation material will be less than in most buildings.

1.3 Aim and innvovations

The aim of this article is to evaluate solutions for improved energy efficiency in a shipping container building. The goal is to work towards ZEB in an off-grid operation. By experiments and simulations, the performance of various designs are investigated. The targeted audience of the paper are architects, engineers working on building design, and HVAC and policymakers, who make regulations to ensure sustainable urban development. Due to the growing need for water supply in urban areas, rainwater harvesting is also investigated. Among the innovations are:

- The change in thermal resistance for a standard container building with 50 mm mineral wool insulation after adding VIPs is verified.

- Studies of different ventilation strategies for container buildings are missing in the literature. Therefore, natural, mechanical, and hybrid ventilation is simulated and compared.
- The relative energy use reduction and Net Present Value of several energy conservation measures are compared.
- Roof Rainwater harvesting is estimated to be able to supply the whole annual water demand in the container building.

2. Materials and Methods

In this study, SketchUp, IDA Indoor Climate, and Energy (IDA ICE) software were used in the process, from developing the first 3D model of the building to simulating the energy need, indoor air quality, and thermal comfort. The floor plan was taken as input in IDA ICE 4.8 [50]. IDA ICE is a whole-year detailed and dynamic multi-zone simulation application for the study of thermal indoor climate as well as for the energy use of an entire building [51]. Building performance was assessed for a typical weather year in Shanghai (IWEC 2.0). The model does not take into consideration the local wind and shading conditions. Also, the energy use connected with equipment use was minimized, assuming that the occupants live a simple lifestyle for economic and environmental reasons.

2.1 Case study

The Shanghai climate entails an average outdoor temperature of 27 °C during the warmest months, while winters can be described as mild, with mean temperatures in the coldest month above 0°C. During the entire year, relative humidity is high, usually over 70%. The challenging summer

conditions engender significant energy use and related GHG emissions connected with cooling and dehumidifying needs, in addition to the heating loads in winter [52].

As can be seen from Figure 1, the south façade of the structure is shaded from the high summer sun, while the heat gain from the low winter sun can be utilized.

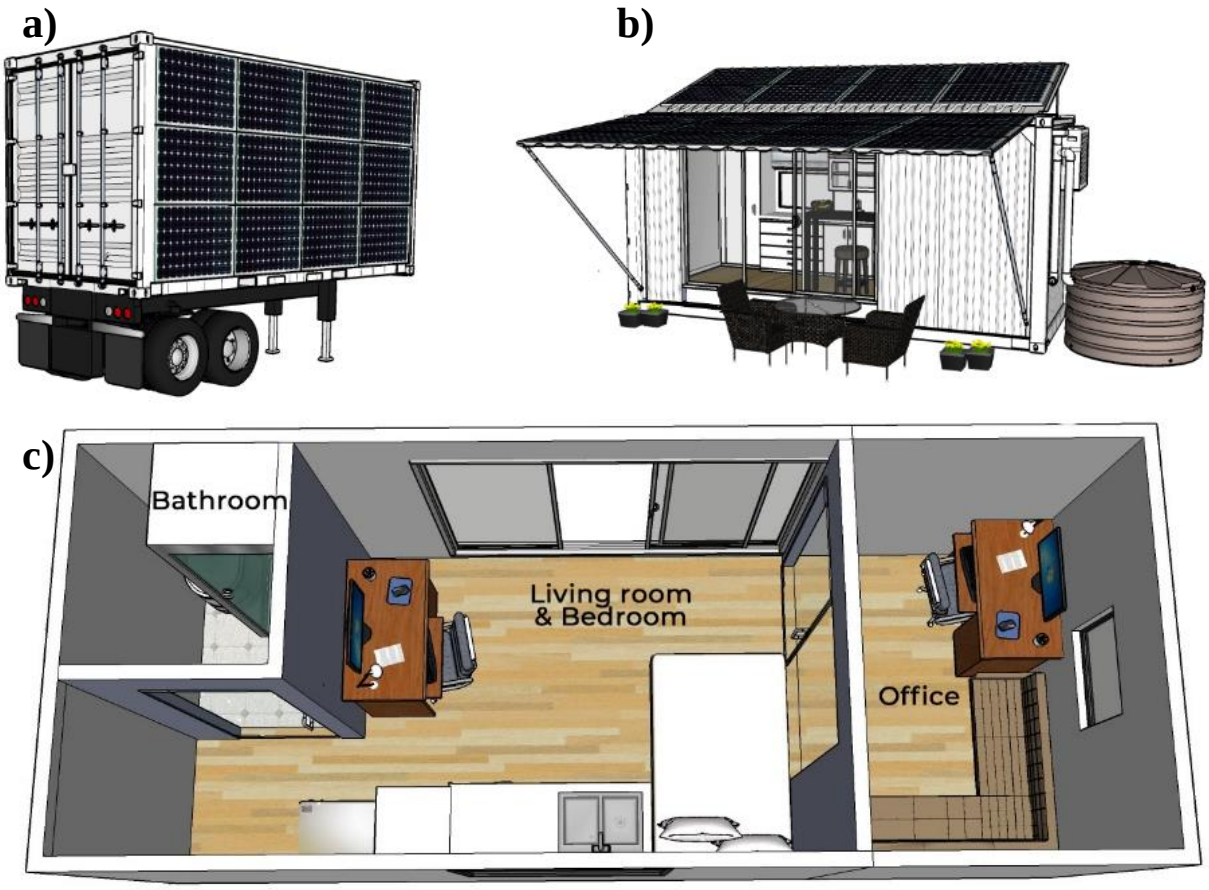

Figure 1. Visualization of the case study building: a) during transportation, b) the south façade, c) top view.

Figure 2. The prototype building as seen at Shanghai Jiao Tong University: a)the south façade, b) inside the living room.

The energy demand for cooling and ventilation was reduced by utilizing cross ventilation through the window and door (Figure 2). The indoor heat pump unit provides the space heating and cooling. To make our building independent of a sewage grid and to save water, a composting Separett waterless toilet was chosen [53]. It is known to be clean and prevent odor [54].

Table 1 presents the most important characteristics of the container building depicted in Figure 2.

Table 1. Container building characteristics.

External dimensions	9m·3m·2.9m
Heated floor area	21 m^2
Internal volume	54.6 m^3
Design occupancy	2 persons that are at home: Weekdays 5 pm-7 am and weekends 6 pm - 12 noon.
Window-to-wall ratio	19 %
Airtightness n_{50}	1/h

SCOP (heating)	2.8
SEER (cooling)	4.4
Electric appliances peak power	800 W

The dehumidification strategy is to lower the heat pump setpoint in order to provide dehumidification when excess PV power is available. A passive solar dehumidification concept based on multilayer moisture-permeable panels was investigated for possible future implementation, but the experimental test was not completed before the construction of the building [55]. The wooden furniture was also chosen to provide a buffer for the humidity. To reduce the accumulation of humidity inside the building from showering, a shower cabinet and extract ventilation from the bathroom was installed.

The PV system has a theoretical peak power of 5.5 kW and consists of 20 solar panels arranged in two rows of ten modules each. A total of 24 lead-carbon batteries were connected in a series, giving the pack an overall capacity of 48V and 24 kWh.

2.2 Experimental activity

2.2.1 Test of VIP performance

To provide input data for the simulation, the thermal resistance of the VIP was measured. To independently test the performance of VIP in a container building, a standard container building was purchased (Figure 3a) and VIP panels were taped to its walls and roof with double-sided tape (Figure 3b). The thermal performance test and energy use analysis was conducted in Shanghai during the winter. The thermal resistance of the standard container building with 50 mm mineral wool insulation and without VIP had previously been verified to 1.0 m^2K/W. According to the

parameters provided by the manufacturer [56], the theoretical thermal resistance of the VIP panels is 2.67 m^2K/W. The total thermal resistance of the wall, R_T, after installing the VIP was therefore expected to be 3.67 m^2K/W. To verify R_T, measurements and calculations were done according to ISO 9869 [57], except that the temperature sensors had an accuracy equal to instead of smaller than 0.5 K, meaning that:

- The temperature difference between the outside and inside was at least 15 degrees (during the VIP testing this was fulfilled 99% of the time, with an average temperature difference of 20.5 °C and a minimum temperature difference of 14.6 °C).
- The sensors were mounted at appropriate locations, investigated by thermography (Figure 3c). The sensors were not under the direct influence of heating or cooling devices or under the draft of a fan.
- The Heat Flow Meter (HFM) was not installed near thermal bridges.
- The surface temperature sensor was mounted close to the HFM.
- The test time exceeded the minimum recommended test duration of 72 h.

By evaluating the average values of the heat flow rate and temperatures over several days and neglecting the hours where direct solar radiation impacts the results, an accurate approximation to steady-state was achieved. Calculations of R_T were done according to the average method in ISO 9869 (Equation 1).

$$R_T = \frac{\sum_{j=1}^{n}\left(T_{si,j} - T_{se,j}\right)}{\sum_{j=1}^{n}\left(q_{si,j} + q_{se,j}\right)/2} \qquad \text{(Equation 1)}$$

where T_{si} is the interior surface temperature of the wall [K]

T_{se} is the exterior surface temperature of the wall [K]

q_{si} is the density of the heat flow rate measured at the interior surface [W/m^2]

q_{se} is the density of the heat flow rate measured at the exterior surface [W/m^2]

j is the measurement number

n is the total number of measurements

It was assumed that there is a negligible lateral heat transfer. Consequently, a heat flow meter could be used to measure R_T. After the installation of VIP, the heat flow rate became low and the signal from the heat flow meter declined towards zero, making small disturbances having a large impact, which can be seen from the large fluctuations in Figure 7. Consequently, better accuracy was obtained by using an average value of the outside and inside heat flow meter and removing the measurements between 7 AM and 5 PM that could be impacted by solar radiation. With additional measurements of the indoor and outdoor wall temperatures, the thermal transmittance of the building element (U-value) was calculated.

The thermal bridges before VIP installation were clear on the thermogram, as shown in Figure 3c, thus it was determined that the installation of VIP could reduce the thermal bridges.

Figure 3. a) Standard container building, b) Test of Vacuum Insulation Panels (VIP) with thermocouples and heat flow meters, c) Thermogram of the walls before the installation of VIP.

Figure 4a shows the makeup of the wall. The sensors were mounted as illustrated in Figure 4b. All sensor data were collected by the data collector Keithley 2700.

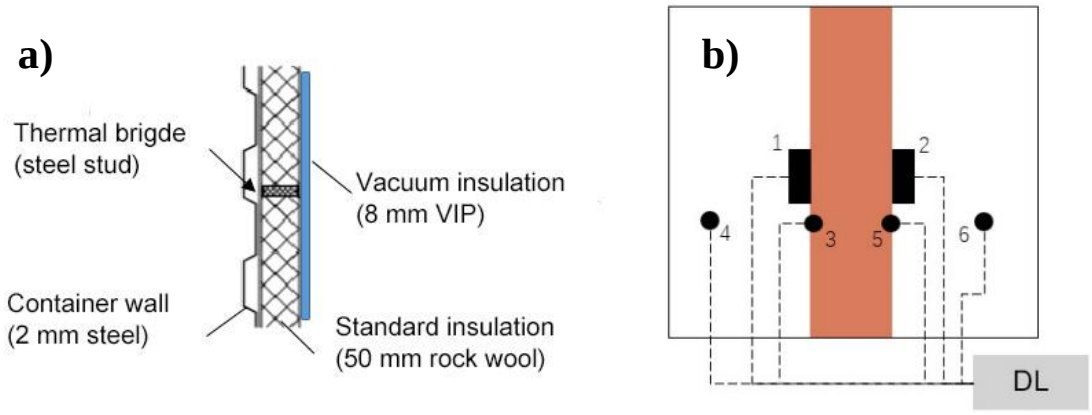

Figure 4. a) Cross section of the wall and placement of sensors, b) The heat flow meters (1 and 2), the surface temperature sensors (3 and 5), and the air temperature sensors (4 and 6).

2.2.2 Validation of the simulation model

The energy model was verified based on monitoring data. Table 2 shows the specifications of the air-to-air heat pump that were used during the test. For the validation, a weather file made from measured weather data from an on-site weather station for the simulated period was used. In addition, the generic model of the air-to-air heat pump in IDA-ICE was adjusted according to performance data provided by the manufacturer. During the VIP experiment, the indoor temperature setpoint was set to 25 °C. It should be noted that this heating setpoint is higher than the ordinary heating setpoint in the building, which is 20 °C, since a 15 °C temperature difference between the outside and the inside had to be obtained.

Table 2. Air-to-air heat pump specifications for GREE KFR-35W/FNhD02-A1 outdoor unit (corresponding to indoor unit model KFR-35GW/(35592)FNhAa-A1)

Cooling power (rated/min./max.)	3500/200/4200 W
Heating power (rated/min./max.)	4900/500/5600 W +1000 W (Additional electrical heating)
Cooling input power (rated/min./max.)	840/90/1300 W
Heating input power (rated/min./max.)	1450/120/1700 W
SEER	5.33
SCOP	3.53
Yearly COP	4.53

Measurements were performed in Shanghai for seven days during the winter in January 2019 as well as for seven days during the summer in July 2019. The measured variables included indoor air temperature at three different heights, heat pump electricity consumption, ambient temperature, solar radiation, wind direction, and wind speed. The relevant parameters of the experimental sensors are shown in Table 3.

Sensor	**Measurement**	**Type**	**Accuracy**

Thermocouple	Wall temperatures and air temperatures in VIP testing in section 5.1	T type	±0.5°C
Heat flow meter	Heat flow through the wall	HF-1A	±3%
Electric meter	Heat pump electricity use	DDSD1352-C	1.0 (approximately 10-20 Wh)
Resistance thermometer	Indoor air temperature for validation of simulation	Pt 100	±0.35°C

Table 3. Sensor parameters.

2.3 Model construction

Table 4 summarizes the design values that were used to simulate the energy need in IDA ICE. The passive house standard for the hot and humid climate [58] was used as a guideline establish stricter demand specifications than the Chinese Residential building energy efficiency standard DGJ 08-205-2015 [59].

Table 4. Demand specifications.

	Passive house standard for hot climate [58]	Chinese standard [59]	Chosen design value
U-value External walls	<=0.50 W/m^2·K	<=0.8 W/m^2·K	0.26 W/m^2·K
U-value for Roof	<=0.50 W/m^2·K	<=0.70 W/m^2·K	0.26 W/m^2·K
U-value for Floor towards ambient air	<=0.50 W/m^2·K	<=2.0 W/m^2·K	0.99 W/m^2·K
U-values for Doors and windows, including the frame	<= 1.25 W/m^2·K	1.8 – 2.2 W/m^2·K	2.8 W/m^2·K
Solar Heat Gain Coefficient (SHGC) of windows	-	-	0.76
Normalized thermal bridge value	<= 0.03 W/m^2·K	-	0.1 W/m^2·K
Air leakage number at 50 Pa	< 0.60/h	< 1/h	1/h

Yearly average temperature efficiency of the heat exchanger *	>= 80 %	-	-
Minimum ventilation humidity recovery rate *	60 % in a humid climate	-	-
SFP	<= 0.5 kW/(m^3/s)	-	-

* Defined in the Appendix.

By applying vacuum insulation panels, acceptable U-values were reached (Table 5), although the passive house standard was not achieved. Due to the limited budget, double glazing windows were used, although triple glazing, with a low g-value was assumed during the conceptual design phase. Figure 5 shows the simulation of the U-value of the wall with symmetric boundary conditions at the short ends in THERM 7.7. The isotherms around the steel framing (black) show that these are thermal bridges. The U-value given in Table 5 includes the effect of the thermal bridges.

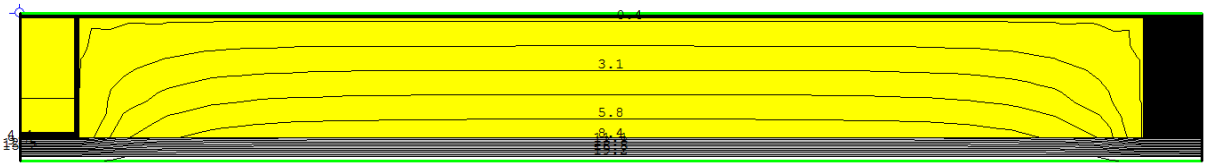

Figure 5. Isoterms for the temperature in the wall between the outside at 0°C and the inside at 20°C. The green lines are the boundary conditions at the inside and outside, the yellow area is the mineral wool insulation, the black area is steel framing and the grey area is the VIP.

Table 5 summarizes the materials and total heat transfer coefficient for the constructed building envelop including floors, roof, and external walls.

Table 5. Building partitions with their total heat transfer coefficient U [W/m^{2}K]

	U [W/m^{2}K]	**Building materials from outside to inside**
Floor	0.99	2 mm steel, 20 mm polyurethane insulation, 20 mm wood, 2 mm PVC
Roof	0.26	2 mm steel, 50mm mineral wool, 8 mm VIP, 3mm bamboo
External wall	0.26	2 mm steel, 50mm mineral wool, 8 mm VIP, 3mm bamboo

A heat pump was used for heating and cooling. The appliance loads, in addition to the heat pump, can be found in Table A.2. The peak power for electric appliances was set to 800 W.

The installed exhaust fan in the bathroom only has an on/off control with a constant airflow rate of 200 m^3/h, which equals 28 $l/(s \cdot m^2)$ or 3.7 ACH. This airflow rate is 98 m^3/h higher than the design airflow rate for this building according to the EU standard EN 16798-1:2019 [60], assuming two persons and a low polluting building. Fresh air is supplied by slightly opening the office window. The air overflows between the rooms through gaps in the doors.

The building was simulated with a heating setpoint of 20 °C and a cooling setpoint of 26 °C. A concentration below 1000 ppm is generally a sign of sufficient air change rate to dilute bioeffluents. Concentrations between 2000 and 5000 ppm are associated with headaches, sleepiness, and stuffy air.

Figure 6 shows the building model from IDA ICE. Wind pressure coefficients based on AIVC recommendations for exposed suburban low-rise building locations. Pressure coefficients for openings were set to 0.75 for windows and 0.65 for internal doors [61]. The number of occupants was set to 2, with a clothing level equal to 1 ± 0.2 clo and an activity level of 1.0 met [1].

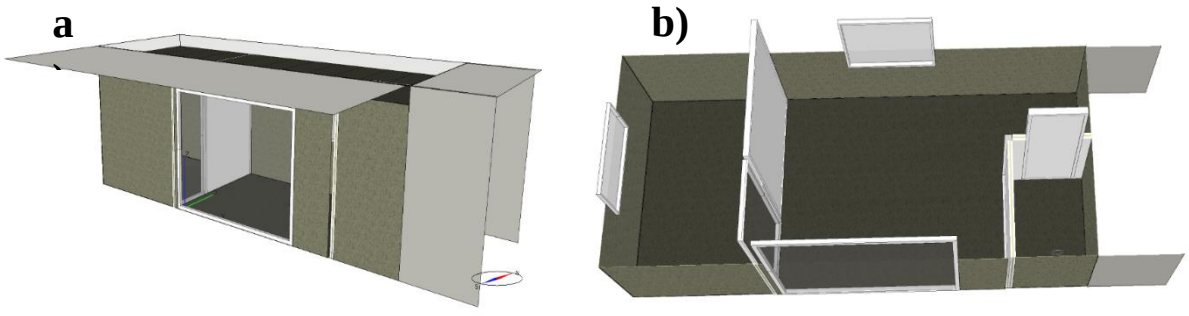

Figure 6. Building model from IDA ICE. a) envelope with shading surfaces b) interior walls and openings.

3. Results

In this section, the experimental results and model validation are first presented. Then simulation is used to evaluate alternative designs and schedules to provide a low energy need that is necessary to achieve off-grid ZEB in real operation but still maintain an acceptable indoor climate.

3.1 Experimental results

The thermal resistance of the building envelope (wall & roof) was increased from 1.0 m^2K/W to around 3.7 m^2K/W (Figure 9a). Because the signal from the heat flow meter declined towards zero after installing the VIP, small disturbances caused large fluctuations, as seen in Figure 7. In comparison, the measurements without VIP were much more stable, and from Figure 8 it can be seen that the thermal resistance was around 1 m^2K/W, as expected.

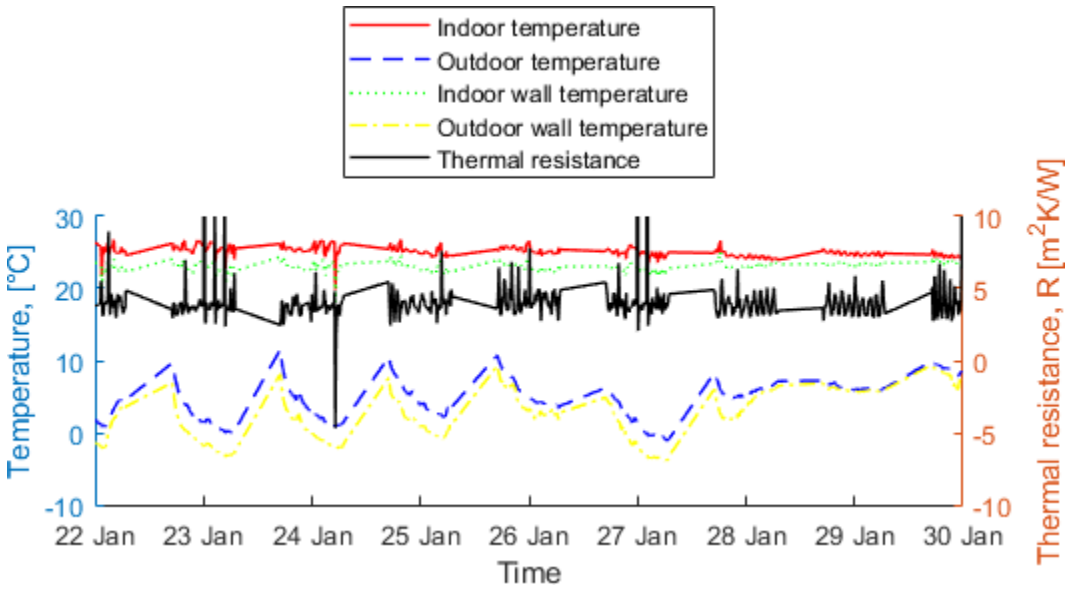

Figure 7. Measured temperatures and calculated thermal resistance for the container wall with VIP, January 22-29, 2019.

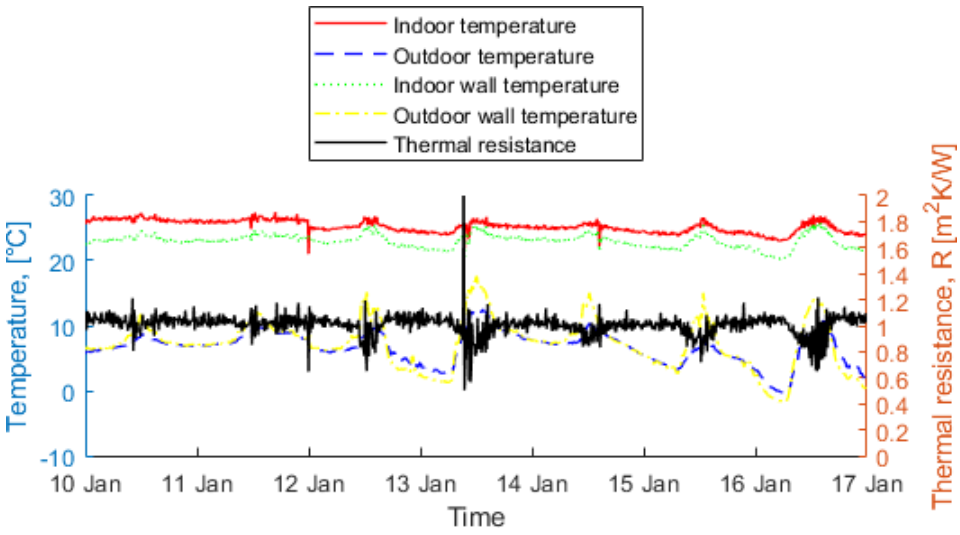

Figure 8. Measured temperatures and calculated thermal resistance without VIP, January 10-17, 2019.

Histograms (Figure 9) were found to be more suitable than the average value in order to determine the trend, so as to avoid the impact of the measurement errors. Figure 9 (a) shows a peak between 3.6 and 3.8 m^2K/W, while Figure 9 (b) shows a peak between 1 and 1.05 m^2K/W.

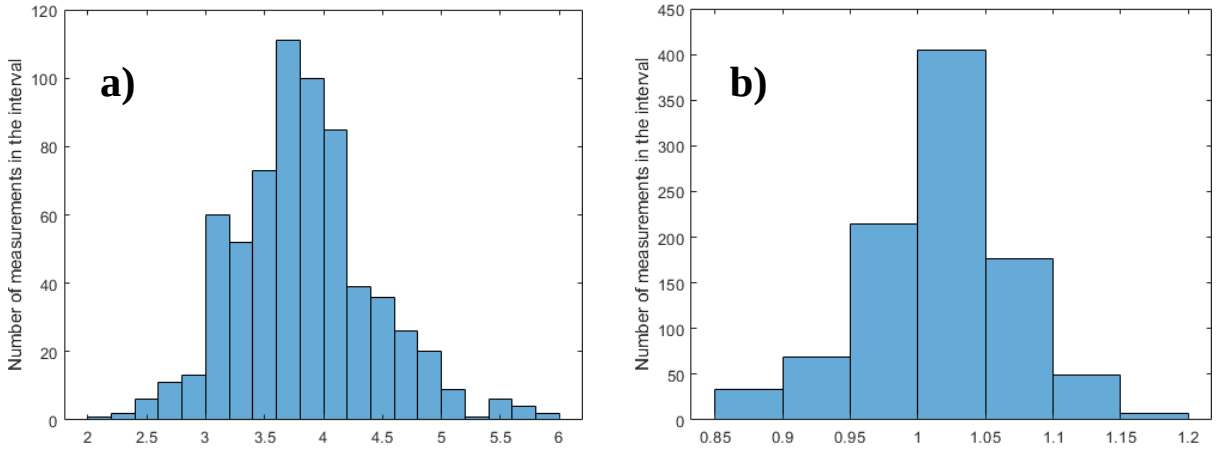

Figure 9. Histograms for the measurements of thermal resistance: a) with VIP, b) without VIP.

The energy use for heating of the container was measured before and after the VIP installation. The relationship between the daily energy use of the heat pump and the average ambient

temperature is shown in Figure 10. It should be noted that environmental factors like solar radiation and wind speed also affect the energy use of the heat pump, but the ambient temperature is the main influencing factor. Figure 10 only considers the effect of ambient air temperature. The energy use before VIP installation is 11.4~16.0 kWh/day, and the average energy use is 13.2 kWh/day. After the installation of VIP, the energy use of the heat pump was 7.0~8.7 kWh/day, and the average energy use was 7.9 kWh/day. Consequently, the average energy use after VIP installation was reduced by about 40%. It can be clearly seen that the temperature dependence of the heating need is much less with VIP.

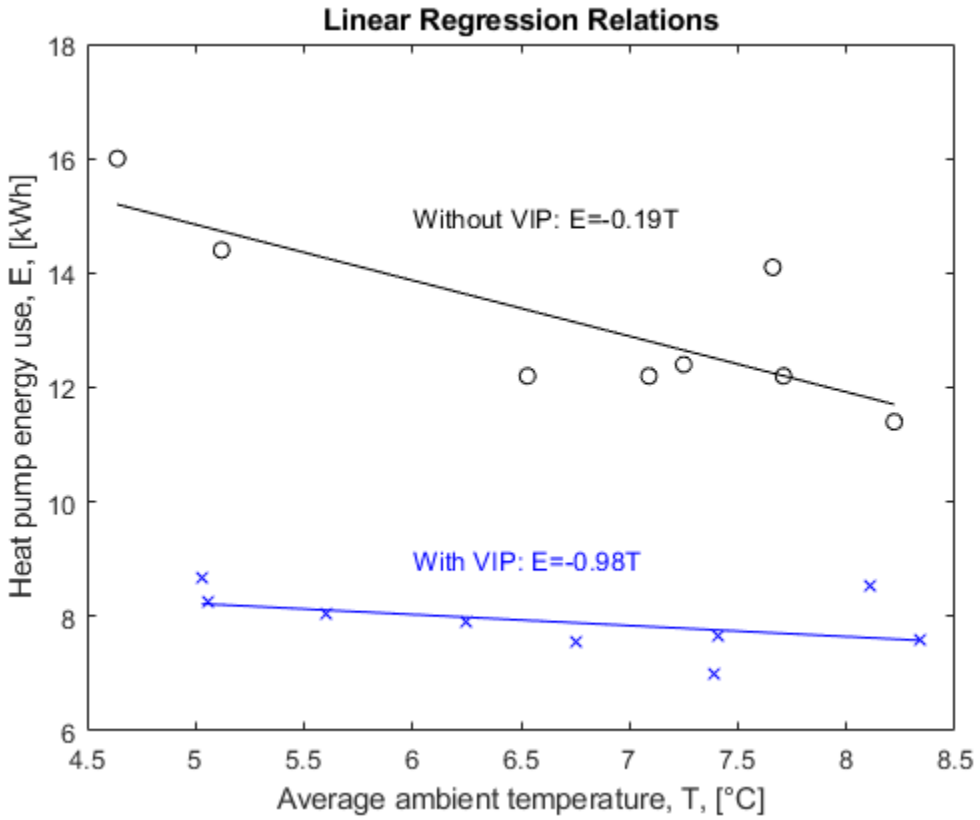

Figure 10. Mean daily energy use with and without VIP as a function of ambient temperature.

3.2 Model validation

Figure 11b presents the differences between simulated indoor temperature (T_s) and measured indoor temperature (T_m) during the space heating period 21.01-27.01 and the space cooling period 18.07-23.07. The time step of the data logging was one hour. The absolute error is below 0.5°C for 85% of the data during the week of measurements in January, while for 67% of the data it is in the range of indoor temperature sensor accuracy of 0.35°C (Figure 11a). The Mean Bias Error (MBE) and Root Mean Square Error (RMSE), defined by Equation 3 and Equation 4, for the same period was 0.13°C and 0.36°C , respectively.

$$\mathrm{MBE} = \frac{1}{n}\sum_{i=1}^{n}(T_{s,i} - T_{m,i}) \qquad \text{(Equation 3)}$$

$$RMSE = \sqrt{\frac{1}{n}\sum_{i=1}^{n}(T_{s,i} - T_{m,i})^2} \qquad \text{(Equation 4)}$$

where

$T_{m,i}$ is the monitored temperature [°C]

$T_{s,i}$ is the simulated temperature [°C]

i is the measurement number

n is the total number of measurements

The measured electricity consumption of the heat pump in the heating mode (57.2kWh) was 5% higher than the simulated one (55.5kWh).

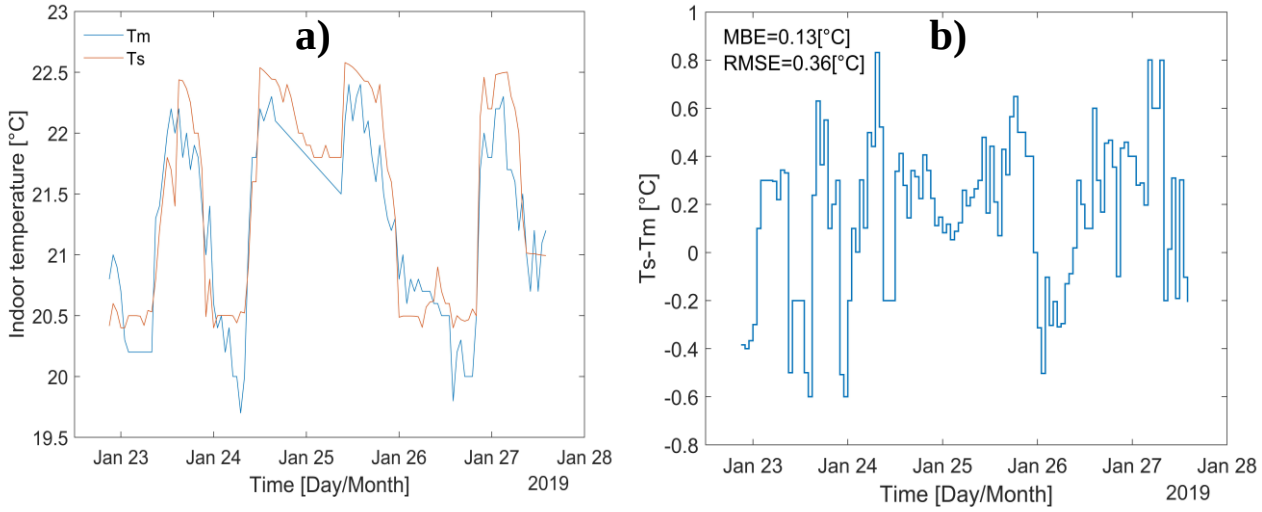

Figure 11 **a) Measured (T_m) and simulated (T_s) indoor temperature a week in January.**

b) Difference between simulated (T_s) and measured (T_m) indoor air temperature.

For the week in July, the differences between simulated and measured indoor air temperature were below 0.5°C for 92% of the data (Figure 12a), while for 78% of the absolute data error is in the range of indoor temperature sensor accuracy of 0.35°C (Figure 12b). For this validation period MBE and RMSE were 0.08°C and 0.28°C respectively. The measured electricity consumption of the heat pump in the cooling mode (31.3 kWh) was 2% higher than the simulated consumption (30.6 kWh).

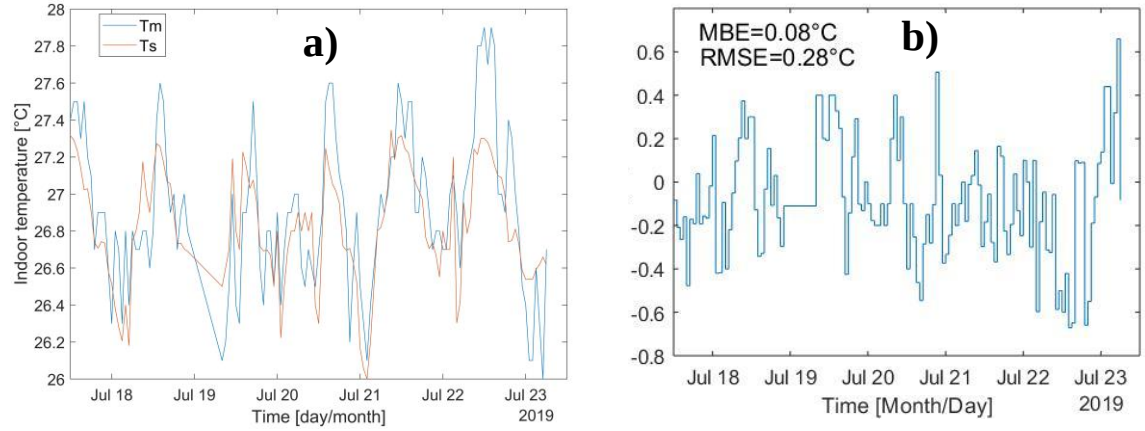

Figure 12. **a) Measured (Tm) and simulated (Ts) indoor temperature during a week in July.**

b) Difference between simulated (Ts) and measured (Tm) indoor air temperature.

3.3 Energy and indoor climate simulation

The simulation results are presented in the following subsections. Before section 3.3.4, only exhaust ventilation is considered, as a base design scenario in the case building in Figure 2. Firstly, in section 3.3.1 the impact of different air change rates on the energy need, peak power, and indoor air quality in the form of the indoor CO_2 concentration are simulated. Secondly, the impact of four different heating and cooling setpoint schedules (Table 10) are analyzed in section 3.3.2. Finally, several possible energy conservation measures, including different ventilation system types, are investigated in sections 3.3.3 and 3.3.4.

3.3.1 The impact of different air change rates

Table 8 presents the different simulated ventilation schedules.

Table 8. Operation conditions and duration of extract fan simulation input.

Schedule	Operation condition	Time period	Duration [h]
Bathroom lights	The bathroom light is on	Sporadically	3
Bedroom	Occupants are sleeping	23:00-07:00	8
Present	Occupants are at home	17:00-07:00	14
Awake	Occupants are in the living room	17:00-23:00	6

The results in Table 9 show that the indoor air quality is clearly best when the extract fan is running whenever there is someone at home. There is little difference in electric energy need for the different schedules, except for heating, since no heat recovery is implemented. During the summer, the cooling need can be reduced mainly by operating the ventilation during the night, when the outdoor temperature is lowest.

Table 9. Simulation results for four different extract fan operation schedules.

	Extract fan operation schedules			
	Bathroom lights	Bedroom	Present	Awake
Indoor environment				
Duration CO_2 < 1000 ppm [h]	3543	3684	8760	5845
Electric energy need				
Heat pump, cooling [kWh]	698	704	797	760
Heat pump, cooling [kWh/m^{2}a]	33	33	37	35
Heat pump, heating [kWh]	594	891 (+50%)	1167 (+96%)	776 (+31%)
Heat pump, heating [kWh/m^{2}a]	28	41	54	36
DHW [kWh]	941	941	941	941
DHW [kWh/m2a]	44	44	44	44
Appliances [kWh]	1032	1032	1032	1032
Appliances [kWh/m^{2}a]	48	48	48	48
Total [kWh]	3265	3568 (+9%)	3937 (+21%)	3509 (+7%)
Total [kWh/m^{2}a]	153	166	183	163
Peak power				
Cooling (C) [kW]	1.02	1.03	1.03	1.03
Heating (H) [kW]	0.99	0.99	1	1
DHW [kW]	0.5	0.5	0.5	0.5
Appliances (A) [kW]	0.35	0.35	0.35	0.35
Total (C + H + DHW + A) [kW]	2.86	2.87	2.88	2.88

For the "Present" schedule, Figure 13 shows that the CO_2 concentration is kept below 800 ppm. The CO_2 level increases rapidly when the extract fan is turned off due to the limited room volume. The concentration is still far from reaching dangerous levels with any of these schedules. However, without an open window, there is likely to be problems with stuffy air, unless the extract fan is on

whenever someone is at home. The “Present” schedule is therefore recommended unless power-saving measures during off-grid operation in the winter require the ventilation to be minimized.

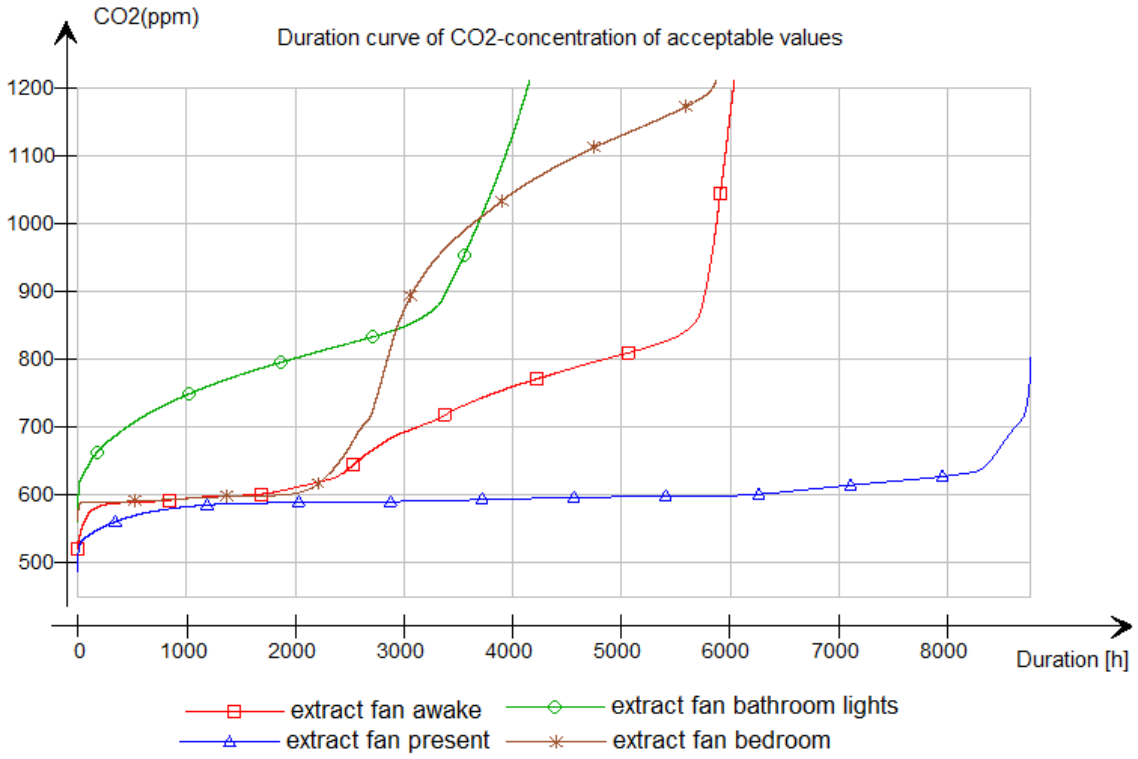

Figure 13. Duration curve of CO2 concentration for four different ventilation schedules.

Figure 14 illustrates that reducing the ventilation rate significantly lowers the energy need as well, but other energy conservation measures that do not limit comfort are preferable.

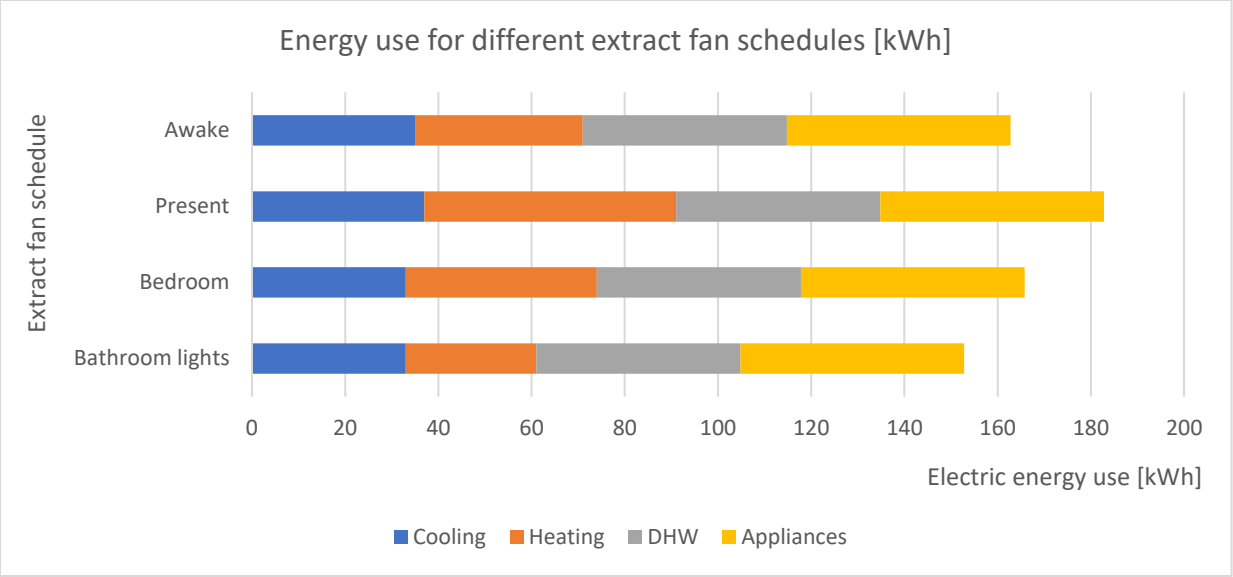

Figure 14 Energy use for four different ventilation schedules.

Figure 15 shows that it is possible to reduce the airflow rate of the extract fan to 68 m^3/h and still keep the CO_2 concentration below 1000 ppm over 7689 hours a year. In comparison, the minimum requirement in the regulations would only provide a sufficient air change rate in less than 3000 hours a year. An airflow rate of 68 m^3/h can be a reasonable compromise between indoor air quality and low energy need for this building, which is needed in order to reach ZEB.

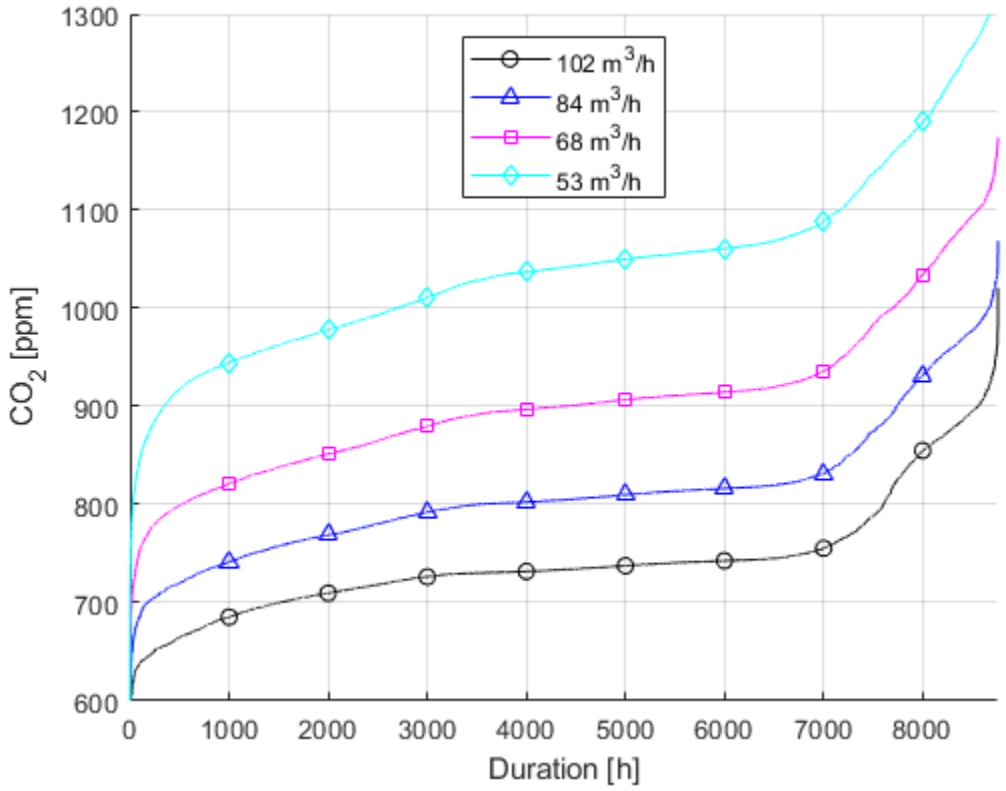

Figure 15. Duration curve for different extract fan airflow rates for the "Present" schedule in Table 8.

3.3.2 The impact of different indoor temperature setpoint schedules

To investigate the impact of the alternative heating and cooling setpoint schedules in Table 10, simulations were done with an air change rate of 68 m^3/h for the "Present" schedule in Table 8. Intermittent heating or cooling is the most typically used operation pattern in China, but a drawback of this operation strategy is that it leads to a higher peak power demand. Intermittent heating or cooling in the case building resulted in temperatures as low as 10°C and as high as 50°C during non-occupancy hours.

Table 10. Heating and cooling setpoints.

Temperature schedule	Cooling setpoint	Heating setpoint
Constant	26 (00:00-24:00)	20 (00:00-24:00)
Energy conservation scenario 1 Wider range of heating and cooling setpoints outside operation hours	**Weekdays** 26 (16:00-07:00) 28 (07:00-16:00) **Weekends** 26 (00:00-24:00)	**Weekdays** 20 (16:00-07:00) 15 (07:00-16:00) **Weekends** 20 (00:00-24:00)
Energy conservation scenario 2 Wider range of heating and cooling setpoints outside operation hours and lower heating setpoint at night	**Weekdays** 26 (16:00-07:00) 28 (07:00-16:00) **Weekends** 26 (00:00-24:00)	**Weekdays** 20 (16:00-22:00) 15 (22:00-16:00) **Weekends** 20 (06:00-22:00) 15 (22:00-06:00)
Energy conservation scenario 3 Heat pump off outside operation hours and lower heating setpoint at night	**Weekdays** 26 (16:00-07:00) Off (07:00-16:00) **Weekends** 26 (00:00-24:00)	**Weekdays** 20 (16:00-22:00) 15 (22:00-07:00) Off (07:00-16:00) **Weekends** 20 (06:00-22:00) 15 (22:00-06:00)

From Table 11 it can be seen that the main effect of the energy conservation scenarios would be the over 40% reduction in energy need for heating in scenarios 2 and 3. This is illustrated in Figure 16. This is reasonable since the average temperature difference between the outdoor temperature and the heating setpoint in winter is much higher than the average difference between the cooling

setpoint and the outdoor temperature in summer. Turning off the heat pump outside operation hours does not have a significant effect on the energy need, but strongly decreases the comfort, because it takes time to readjust the indoor temperature to the setpoint. Therefore, it is recommended to increase the temperature range outside operation hours, as in Scenario 2, unless energy shortage due to low forecasted PV generation is expected. All three scenarios increase the total peak power by 14-18%. This may require an inverter with higher capacity, but that does not significantly impact the cost of the energy system, which is mainly decided by the PV and battery capacity.

Table 11 Simulation results for alternative heating and cooling setpoint schedules with relative changes compared to constant setpoint in percentage.

	Constant setpoint	Scenario 1	Scenario 2	Scenario 3
Electric energy need				
Heat pump, cooling [kWh]	735	693 (-6%)	693 (-6%)	661 (-10%)
Heat pump, cooling [kWh/m^{2}a]	35	33	33	31
Heat pump, heating [kWh]	755	671 (-11%)	446 (-41%)	440 (-42%)
Heat pump, heating [kWh/m^{2}a]	36	32	21	21
DHW [kWh]	941	941	941	941
DHW [kWh/m^{2}a]	44	44	44	44
Appliances [kWh]	1032	1032	1032	1032
Appliances [kWh/m^{2}a]	48	48	48	48
Total [kWh]	3463	3337 (-4%)	3112 (-10%)	3074 (-11%)
Total [kWh/m2a]	163	157	146	144
Peak power				
Cooling (C) [kW]	0.83	1.01 (+22%)	1.01 (+22%)	1.06 (+28)
Heating (H) [kW]	0.88	1.05 (+19%)	1.10 (+25%)	1.10 (+25%)
DHW [kW]	0.5	0.5	0.5	0.5

Appliances (A) [kW]	0.35	0.35	0.35	0.35
Total (C + H + DHW + A) [kW]	2.56	2.91 (+14%)	2.96 (+16%)	3.01 (+18%)
Comfort category				
(EN-15251, with cooling)		No. of occupancy hours		
I (best)	408	408 (+0%)	399 (-2%)	349 (-14%)
II (good)	827	827 (+0%)	825 (+0%)	742 (-10%)
III (acceptable)	2364	2364 (+0%)	2646 (+12%)	2488 (+5%)
IV (unacceptable)	136	136 (+0%)	124 (-9%)	282 (+107%)

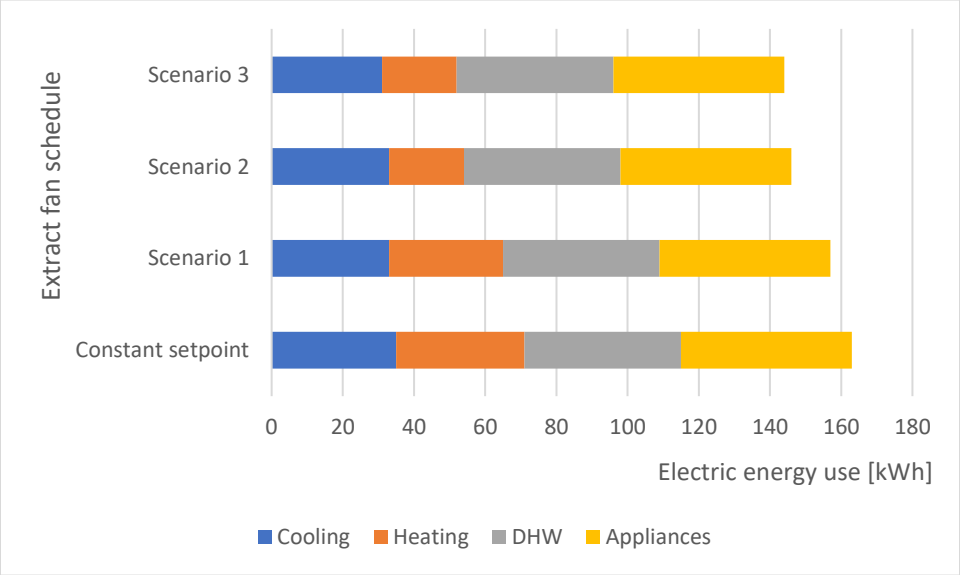

Figure 16. Energy use for different heating and cooling setpoint schedules.

Table 11 indicates that the indoor temperature falls outside the comfort range for part of the year. This probably occurs primarily when the occupants are sleeping during the winter, when they will have an insulation level higher than the standard indoor winter clothing that is assumed for the comfort simulation. Therefore, the occupants will likely not feel uncomfortable. Comfort category IV in Table 11 is based on EN-15251 reference values and occurs when the indoor operative

temperature is lower than 18 °C during the heating season or higher than 26 °C during the cooling season.

3.3.3 Suggested energy conservation measures

Table 12 presents various energy conservation measures that can reduce energy requirements. Particularly for off-grid buildings, these energy conservation measures can be cost effective because they reduce the need for investment in energy generation and storage capacity. Unless another reference is mentioned in the table, the impact of each energy conservation measure is provided, with reference to the built container building in Figure 2, with constant temperature setpoints according to Table 10 and an air change rate of 68 m^3/h for the "Present" schedule in Table 8. The peak power remains unchanged at 3.01 kW due to the fact that the heat pump's maximum heating and cooling power is reached in all cases.

Lowering the U-values of the façade to 0.1 W/m^2K, for instance by tripling the VIP thickness to 24 mm, reduces the energy need for heating by 36% without reducing the floor area significantly. Reduction of the door width does not significantly contribute to reducing the heating requirement, since the windows also provide passive heating during the winter. However, reducing the width of the door makes it possible to place the door at the short end of the container. Thus the construction process might be simpler, since the container doors on the short end often must be replaced if a container is to be modified into a building. The energy and work required for strengthening the walls of the container to maintain its structural strength after cutting an opening will thereby be saved. A smaller window area towards the south that maintains good daylight conditions, while reducing the heat loss, is recommended in climates with cold winters. By upgrading to triple glazing with argon filling the U-value of the windows can be reduced to 0.7 W/m^2K. The price for such windows is around 4000 ¥/m^2 and they are around 25% more expensive than traditional

double layer glazing windows with air in the glazing gap. This energy conservation measure has a high impact on reducing both heating and cooling. Lastly, the reduction of the air change rate down to the Chinese standard can help to reduce the heating need and may, therefore, be an option during the coldest seasons.

Table 12. Proposed energy conservation measures and impacts compared to the built reference case building.

Description	**Electric energy need for heating**		**Electric energy need for cooling**	
	[kWh/m^{2}a]	**Impact**	**[kW]**	**Impact**
Improved insulation				
Base case (ref.)	21.2		31.5	
All surfaces U=0.2 W/m^{2}K	16.4	-23%	29.6	-6%
All surfaces U=0.15 W/m^{2}K	15.1	-29%	29.4	-7%
All surfaces U=0.1 W/m^{2}K	13.6	-36%	29.4	-7%
Reduced door width				
2.5m	20.4	-4%	31.5	-4%
2m	19.9	-6%	31.7	-5%
1.5m	19.4	-8%	29.8	-10%
Better windows				
U=1.9 W/m^{2}K g=0.68	16.8	-21%	32.8	-1%
U=1.1 W/m^{2}K g=0.56	14.6	-31%	31.7	-4%
U=0.7 W/m^{2}K g=0.36	15.3	-28%	28.8	-13%
Reduced extract air flow rate				
53 m^3/h (CN)	19.9	-10%	31.8	-4%

3.3.4 Evaluation of energy need for natural, hybrid and mechanical ventilation scenarios

To investigate whether a different ventilation strategy could further reduce the energy requirement, three different systems were simulated: Natural ventilation (NV), mechanical ventilation with heat recovery (MV), and hybrid ventilation (HV). Hourly load profiles were evaluated. The evaluation of the indoor air quality was limited to monitoring the CO_2 concentration in the office and living room. To meet the requirements of China's Indoor Air Quality standards, the upper limit was set to 1000 ppm [62]. In addition, the outdoor concentration was set to 400 ppm, and each person was assumed to generate 18 l/h of CO_2 [63].

3.3.4.1 Natural ventilation (NV)

In the NV scenario, windows in the living room and office were opened to one-quarter of their maximum openable range when the indoor concentration of CO_2 in the occupied zone exceeded a value of 1000ppm. The windows were shut when the indoor in-zone temperature fell below 16 °C during space heating periods or when temperatures exceeded 28°C during space cooling periods. The hysteresis value of opening and closing windows was set at 300 ppm of indoor CO_2 concentration. If windows were closed, infiltration airflow was based on leak sizes, wind pressure and thermal buoyancy effects. The annual average infiltration rate was approximately 0.4 air changes per hour (ACH) when all windows were shut. Wind pressure coefficients were based on data recommended for low-rise buildings with exposed, suburban location and a length-to-width dimension ratio of 3:1 [64].

3.3.4.2 Mechanical ventilation with heat recovery (MV)

In the MV ventilation scenario, no windows were opened in spite of free-cooling conditions. The system was characterized as constant and balanced with a total airflow of 60 m^3/h and supply air rates of 40 m^3/h in the living room and 20 m^3/h in the office. The exhaust air outlets were placed

in the bathroom (40 m^3/h) and office (20 m^3/h). The utilized MV contained a heat recovery system with a rated thermal efficiency of 75%. Power consumption for fans was estimated at 0.5 W/(m^3/h) according to standard Chinese ventilation system data. Note that MV was only operational during building occupancy.

3.3.4.3 Hybrid ventilation (HV)

The HV system was based on infiltration flow when indoor CO_2 concentration was below the zonal threshold of 1000 ppm. Otherwise, the system switched to MV mode.

A summary of the simulation results is presented in Table 13. The heat exchanger particularly reduces the energy need for heating for mechanical and hybrid ventilation. However, the recovered energy is outweighed by the increase in energy need for fans for mechanical ventilation.

Table 13. Energy need and change compared to the base case for alternative ventilation strategies.

	Ventilation scenario			
	Base case Exhaust 68 m^3/h	**NV**	**MV**	**HV**
Electric energy need				
Heating (H) [kWh]	440	516 (+17%)	332 (-25%)	319 (-28%)
Heating (H) [kWh/m^2a]	21.2	24.0	15.4	14.8
Cooling (C) [kWh]	693	694 (+0%)	638 (-8%)	645 (-7%)
Cooling (C) [kWh/m^2a]	33.0	32.6	29.7	30
Fan (F) [kWh]	41.7	0 (-100%)	159.8 (+283%)	112.2 (+169%)
Total (H+C+F) [kWh]	1175	1210 (+3%)	1130 (-4%)	1076 (-8%)
Peak power				
Heating [kW]	1.1	1.07 (-3%)	1.07 (-3%)	1.07 (-3%)
Cooling [kW]	1.06	1.06	1.06	1.06

Hybrid ventilation has the lowest total final electricity consumption, 11% lower than for natural ventilation. The minor annual differences among the total final electricity consumption for all scenarios call into question the economic viability of implementing mechanical or hybrid systems with heat recovery based on the NPV calculation in Table 14. Maintenance and installation costs would further reduce this. Natural ventilation is therefore suggested from an economic point of view. The opening of windows can also provide the proper indoor CO_2 concentration in occupied rooms during the entire year, despite twenty hours with no wind conditions [13].

3.3.5 Economic consideration

To evaluate some of the suggested energy conservation measures, the Net Present Value (NPV) of the investments are calculated according to Equation 5 with a discount rate of 4 % and an electricity price of 2.7 ¥/kWh. The high electricity price is due to the high cost for batteries and PV and is calculated in HOMER Pro [65] based on the market price for the current PV-battery system used in the demonstration building.

$$NPV = S\frac{1-(1+i)^{-n}}{i} - I \qquad \text{(Equation 5)}$$

where S is the annual energy cost savings

i is the discount rate

n is the economic lifetime

I is the additional initial investment

Table 14 presents the potential savings from three of the evaluated energy-saving measures. Because the initial energy use is already low, the annual energy cost savings due to the energy saving measures are also low. Consequently, the investments are unprofitable, unless the installed battery and PV capacity can be reduced. Improved windows are the most profitable option, but is

still not cost effective since the investment is higher than the NPV of the annual savings. Here all 9.9 m^2 with windows and glass doors are replaced.

Table 14. Net Present Value of three suggested energy-saving measures.

Description of measure	Yearly energy cost before the measure [¥]	Yearly energy cost after the measure [¥]	Annual energy cost savings [¥]	Investment [¥]	Economic lifetime [years]	NPV [¥]
Add ventilation system	3267	2905	362	16784 *	20	-11867
Add 16 mm VIP	2906	2371	535	26750 **	25 [66]	-18394
Windows U=0.7 W/m^2K	2906	2432	474	9876 ***	25	-2468

* Flexit C2 REL air handling unit. Mean annual temperature efficiency of 80% in Shanghai at 150 m^3/h. ** 250 ¥/m2 *** 4000 ¥/m2

Based on these results, another solution would be to reduce the window area in order to reduce the investment cost. Even the best windows we have suggested have far higher U-value than the wall, so this will contribute to significant savings. An alternative design is sketched in Figure 17.

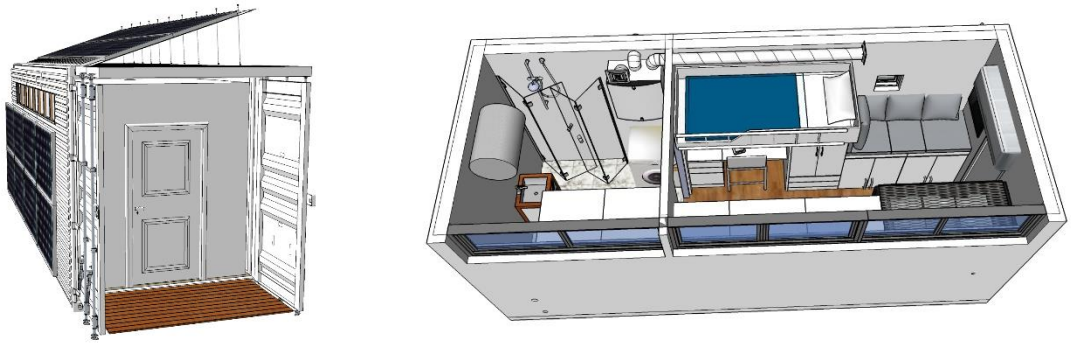

Figure 17. Alternative design with daylight windows at the south façade.

3.4 Potential for rainwater harvesting

Lastly, to investigate the possibility of water self-sufficiency, the potential for water harvesting is briefly evaluated. Zhou and Tol [67] found that the mean annual water consumption per capita varies from about 26 m^3/person in Shanxi province to 107 m^3/person in Shanghai. Water consumption is influenced by the characteristics of an individual as well as the efficiency of showerheads and tap fittings [68]. In homes, around 25% of the water is used for toilet flushing [24]. By assuming a restrictive use of water, equal to that of Shanxi and withdrawing 25% since a composting toilet does not use water, we can estimate a yearly consumption of 20 m^3/person, which equals 55 liters per day.

Shanghai has a high mean annual precipitation of 1200 mm. Filter efficiency is specified by the manufacturer, commonly 90%. For the container building in Figure 1-2, if both roof surfaces are used for water harvesting and the drainage coefficient is 85% for a metal roof with PV panels, there is a potential to harvest 25 m^3/year for the 27 m^3 roof or 50 m^3/year if the shading roof is used as well. A study by Zhang, et al. [69] projects that the mean annual rainfall in China is going to increase by 2.7%–62.0% in the period 2020–2050, due to climate changes, leading to an increased potential.

4. Conclusions

This article has evaluated alternative solutions to improve energy efficiency in order to prepare a solar-powered shipping container building for off-grid operation. VIP is proven to have an excellent insulation performance, although the fragile design and the high price is currently a concern.

Key results include:

- A full-scale experiment showed that the thermal resistance of a container building envelope increased from 1.1 m^2K/W to 3.7 m^2K/W by applying 8 mm VIP insulation.
- Natural ventilation can provide comparable indoor air quality as mechanical ventilation with heat recovery for the described case study, with only 7% higher annual energy need for heating, cooling, and ventilation.
- Hybrid ventilation has the lowest energy need, but for a single container building in a subtropical climate, the 11% difference compared to natural ventilation is not large enough to justify the investment based on a Net Present Value evaluation of the annual savings.
- Upgrading from double to triple glazing windows or reducing the window area was the most economical way of improving the energy performance of the case study building.
- Roof rainwater harvesting may be able to cover the entire need for water for the container home in Shanghai, although it is recommended to purchase drinking water.

Based on these results, further research should investigate control strategies and the inclusion of thermal storage to optimize the utilization of the PV generation. Subsequently, off-grid operation should be simulated and tested. How micro-grids with other energy sources can reduce the investment in the off-grid energy system should also be investigated. Improved strategies for dehumidification would also be important to secure a healthy indoor climate. In future research on ventilation of container buildings, the impact of outdoor Particular Matter (PM) should be included, together with possible filtration methods. A Life Cycle Assessment (LCA) should also be performed in order to compare the emissions for construction and building materials from this

design compared to a conventional building. Finally, an LCA study of modular, container buildings in China, particularly with the off-grid energy-system design scenario, seems to be missing in the literature.

Appendix

"Yearly average temperature efficiency of the heat exchanger" of 80% means that 80% of the energy is recovered from the exhaust air over the year, which reduces the need for heating and sensible cooling through the heat pump in our case.

$$\eta_T = \frac{t_{rec} - t_o}{t_e - t_o}$$

where t_{rec} is the supply air temperature after the heat exchanger [ºC]

t_e is the exhaust temperature [ºC]

t_o is the outdoor air temperature before the heat exchanger [ºC]

For application in warm and humid climates, the use of heat exchangers with moisture recovery is recommended in order to reduce the entry of moisture into the home from outside and related energy related to latent cooling and dehumidification needs.

Minimum ventilation humidity recovery rate of 60 % means that the heat exchanger be able to remove a minimum of 60% of the moisture from the supply air by transferring it to the extract air to reduce the need for dehumidification (from the heat pump in our case).

$$\eta_x = \frac{x_o - x_{rec}}{x_o - x_{ext}}$$

where x_{rec} is the absolute humidity of supply air after the heat exchanger

x_{ext} is the absolute humidity of the extract air

x_o is the absolute humidity of outdoor air before the heat exchanger

Table A.1 presents the most relevant related studies found in the literature, which focus on low energy need, passive solutions for heating or cooling, indoor climate or life cycle assessment. All these factors are important in order to achieve a sustainable ZEB building.

Table A.1. Case studies of residential buildings related to container buildings (* Simulations (S), Experiments (E), Life cycle assessment (LCA)).

Author and year	**Building type and climate according to Köppen-Geiger classification [70]**	**Location**	**Assessment method ***	**Learning outcomes and comments related to the project**
Tavares, et al. [8] 2019	One-story house. Dry-summer subtropical climate (Csb).	Aveiro, Portugal and 7 simulated locations	S (simulation), E (experiment) , LCA	Evaluation of alternative structure materials. Focus on the embodied emissions (EE). The results are impacted by the 100 years estimated lifetime, significantly longer than most studies. Light steel or timber framing has the lowest GHG and EE emissions, compared with traditional concrete or steel-based structures. Operational energy, ventilation or thermal comfort is not considered.
Dara and Hachem-Vermette [71] 2019	Single-family house made from upcycled shipping containers. Continental Subarctic Climate (Dfc).	Calgary, Canada	S, LCA	The operational phase contributed to 85-95 % of the life cycle impacts. Over a 50 years lifespan upcycling steel-based shipping containers and reusing them for housing caused lower environmental impact than a wood-based housing. Upcycling a 12.2 meter shipping container could save 8000 kWh that would be needed to melt and re-manufacture the steel. In 2018 there were enough leftover containers in Canada to cover 18% of the need for single-detatched houses.
Taleb, et al. [33], 2019	Container home in a subtropical desert climate (BWh)	Aswan, Egypt	S, E	Green roofs and green walls were used to act as an insulation layer for the container envelope. Triple glazing windows with low-emissivity film played a key role in reducing the cooling load.

Bohm [29], 2018	Container building in a warm, humid climate (Dfb).	Buffalo, USA	S, E	Thick walls, modest windows, structurally insulated panels with little thermal bridging, triple-panel windows with low-e coating. Natural ventilation with manually operated wooden hatches that are closed and filled with insulation during the winter. Good thermal comfort due to airtight and well-insulated envelope and separate thermal zones.
Tumminia, et al. [10] 2018	One-story NZEB office building with a container-like structure in warm summer and cold winter climate (Csa).	Sicilia, Italy	S, E, LCA	Low emissivity windows, lights controlled by illuminance dimming and presence sensor. Use natural ventilation, but it is found to be undesirable during the warm summer and limited during the cold winter due to thermal comfort. Materials use contributes to 72% of the total environmental impacts and are recommended to be given more attention.
Cornaro, et al. [30] 2017	Container building in a semi-arid, cold climate (BSk).	Irvine, USA	S, E	Patio with shading of the south façade. Solar chimney for natural ventilation.
Elrayies [36] 2017	Single story building in a tropical and subtropical desert climate (Bwh)	Port Said, Egypt,	S	5 models with different insulation levels. Closed-cell spray polyurethane foam was found to provide the best thermal comfort, followed by straw. Crossflow natural ventilation. Thermal comfort studied according to EN 15251:2007. The thermal comfort was unacceptable 20-55 % of the time, depending on 7 simulated locations.
Wang, et al. [31] 2016	Zero Energy solar house in a semi-arid, cold climate (BSk).	Datong, China	S, E	Adjustable shading, natural ventilation, heat storage, atrium, double layer roof with south overhang, PCM, night cooling. Thermal comfort through controllable shading and ventilation with the atrium as a buffer zone.
Islam, et al. [37] 2016	Double-story home with container structure in a temperate climate (Cfb).	Mel-bourne, Australia	S, LCA	Doubles the building width to 4.9 m by connecting two standard 40-inch (12.2 m) containers horizontally. Use low emissivity windows. The study does not discuss ventilation and thermal comfort. More than 17 million used shipping containers are available globally and reusing them for buildings saves materials and reduce embodied emissions.
Irulegi, et al. [23] 2014	Solar house ($54m^2$) with ventilation (90 % energy recovery in warm summer and cold winter climate (Csa).	Madrid, Spain	S, E	Prefabricated Cross Laminated Timber (CLT) structure. Highly insulated walls, shading and cross-ventilation during the summer, solar heat gain during the winter, thermal mass and PCM to flatten the temperature peaks. Hybrid ventilation, mainly cross-ventilation.
Vijayalaxmi [32] 2010	One-story home with container structure in hot and humid climate (Aw).	Chennai, India	E	Energy conservation from natural ventilation (comfort ventilation), building orientation and shading from trees. 59 % reduction in embodied energy due to the reuse of a shipping container, which was upgraded with an extra cement roof with overhang. The same average indoor temperature as in a traditional building.

Table A.2 presents the load of the container building, in addition to the heat pump. Based on calculations that assume water-saving taps and an efficient use of hot water in order to live off-grid, the daily energy need for hot water for handwashing, showering and cleaning for two persons is estimated to be 3 kWh/day with a peak load of the electric water heater of 500 W and an efficiency of 0.96.

Table A.2. Rated power and duration of the use for the technical equipment and lighting.

Internal loads	**Power [W]**	**Duration per day [h]**
Booster pump	100	1
Laptop	90	8
Fridge	13	24
Exhaust fan from composting toilet	3	24
Extract fan, bathroom	8	Not set
LED lights, living room	10	6
LED lights, bathroom	10	3
LED lights, office	10	3
Crock-pot (slow cooker)	100	8
Electric water heater	500	6
Other plug loads	73	24

Acknowledgments

This paper has been written with funding support from NSFC (51521004) and support from the Research Council of Norway and several partners through the Research Centre on Zero Emission Neighborhoods in Smart Cities (FME ZEN).

Declarations of interest

None

References

[1] *ISO 7730:2005(E) Ergonomics of the thermal environment-Analytical determination and interpretation of thermal comfort using calculation of the PMV and PPD indices local thermal comfort criteria*, ISO, 2005.

[2] I. Sarbu and C. Sebarchievici, "Chapter 2 - Vapour Compression-Based Heat Pump Systems," in *Ground-Source Heat Pumps*, I. Sarbu and C. Sebarchievici Eds.: Academic Press, 2016, pp. 7-25.

[3] W. Ferdous, Y. Bai, T. D. Ngo, A. Manalo, and P. Mendis, "New advancements, challenges and opportunities of multi-storey modular buildings – A state-of-the-art review," *Engineering Structures*, vol. 183, pp. 883-893, 2019/03/15/ 2019, doi: https://doi.org/10.1016/j.engstruct.2019.01.061.

[4] IEA, *World Energy Outlook 2016*. IEA, 2016.

[5] A. B. Kristiansen, T. Ma, and R. Z. Wang, "Perspectives on industrialized transportable solar powered zero energy buildings," *Renewable and Sustainable Energy Reviews*, vol. 108, pp. 112-124, 2019/07/01/ 2019, doi: https://doi.org/10.1016/j.rser.2019.03.032.

[6] P. C. Hui Ling, C. S. Tan, and A. Saggaff, "Feasibility of ISO shipping container as transitional shelter-a review," *IOP Conference Series: Materials Science and Engineering*, vol. 620, p. 012056, 2019/11/19 2019, doi: 10.1088/1757-899x/620/1/012056.

[7] C. Dara, C. Hachem-Vermette, and G. Assefa, "Life cycle assessment and life cycle costing of container-based single-family housing in Canada: A case study," *Building and Environment*, vol. 163, p. 106332, 2019/10/01/ 2019, doi: https://doi.org/10.1016/j.buildenv.2019.106332.

[8] V. Tavares, N. Lacerda, and F. Freire, "Embodied energy and greenhouse gas emissions analysis of a prefabricated modular house: The “Moby” case study," *Journal of Cleaner*

Production, vol. 212, pp. 1044-1053, 2019/03/01/ 2019, doi: https://doi.org/10.1016/j.jclepro.2018.12.028.

[9] C. McConnell and C. Bertolin, "Quantifying Environmental Impacts of Temporary Housing at the Urban Scale: Intersection of Vulnerability and Post-Hurricane Relief in New Orleans," *International Journal of Disaster Risk Science*, vol. 10, no. 4, pp. 478-492, 2019/12/01 2019, doi: 10.1007/s13753-019-00244-y.

[10] G. Tumminia, F. Guarino, S. Longo, M. Ferraro, M. Cellura, and V. Antonucci, "Life cycle energy performances and environmental impacts of a prefabricated building module," *Renewable and Sustainable Energy Reviews*, vol. 92, pp. 272-283, 2018/09/01/ 2018, doi: https://doi.org/10.1016/j.rser.2018.04.059.

[11] E. Ginelli, G. Pozzi, G. Lazzati, D. Pirillo, and G. Vignati, "Regenerative Urban Space: A Box for Public Space Use," in *Regeneration of the Built Environment from a Circular Economy Perspective*: Springer, 2020, pp. 137-147.

[12] E. Ginelli, C. Chesi, G. Pozzi, G. Lazzati, D. Pirillo, and G. Vignati, "Extra-Ordinary Solutions for Useful Smart Living," in *Regeneration of the Built Environment from a Circular Economy Perspective*: Springer, 2020, pp. 347-356.

[13] A. B. K. Daniel Satola, Jakub Dziedzic, Arild Gustavsen, "Assessing the annual power reliability of a residential building in relation to its ventilation system type: The case study of the off-grid container house in Shanghai," *IOP Conf. Ser.: Mater. Sci. Eng.*, vol. 609, no. 072065, 2019.

[14] W. Bowley and P. Mukhopadhyaya, "A sustainable design for an off-grid passive container house," *International review of applied sciences and engineering*, vol. 8, no. 2, pp. 145-152, 2017.

[15] X. Cao, X. Dai, and J. Liu, "Building energy-consumption status worldwide and the state-of-the-art technologies for zero-energy buildings during the past decade," *Energy and Buildings*, vol. 128, pp. 198-213, 2016/09/15/ 2016, doi: https://doi.org/10.1016/j.enbuild.2016.06.089.

[16] D. D'Agostino and D. Parker, "A framework for the cost-optimal design of nearly zero energy buildings (NZEBs) in representative climates across Europe," *Energy*, vol. 149, pp. 814-829, 2018/04/15/ 2018, doi: https://doi.org/10.1016/j.energy.2018.02.020.

[17] S. Attia *et al.*, "Overview and future challenges of nearly zero energy buildings (nZEB) design in Southern Europe," *Energy and Buildings*, vol. 155, no. Supplement C, pp. 439-458, 2017/11/15/ 2017, doi: https://doi.org/10.1016/j.enbuild.2017.09.043.

[18] L. Wells, B. Rismanchi, and L. Aye, "A review of Net Zero Energy Buildings with reflections on the Australian context," *Energy and Buildings*, vol. 158, pp. 616-628, 2018/01/01/ 2018, doi: https://doi.org/10.1016/j.enbuild.2017.10.055.

[19] Wikipedia. "Port of Shanghai." https://en.wikipedia.org/wiki/Port_of_Shanghai (accessed 31.07., 2017).

[20] A. A. P. Olivares, "Sustainability in Prefabricated Architecture: A Comparative Life Cycle Analysis of Container Architecture for Residential Structures: a Thesis Submitted to the Victoria University of Wellington in Fulfilment of the Requirements for the Degree of Master of Architecture," Victoria University of Wellington, 2010.

[21] Y. Chang, X. Li, E. Masanet, L. Zhang, Z. Huang, and R. Ries, "Unlocking the green opportunity for prefabricated buildings and construction in China," *Resources, Conservation and Recycling*, vol. 139, pp. 259-261, 2018/12/01/ 2018, doi: https://doi.org/10.1016/j.resconrec.2018.08.025.

[22] H. Zhu, J. Hong, G. Q. Shen, C. Mao, H. Zhang, and Z. Li, "The exploration of the life-cycle energy saving potential for using prefabrication in residential buildings in China," *Energy and Buildings*, vol. 166, pp. 561-570, 2018/05/01/ 2018, doi: https://doi.org/10.1016/j.enbuild.2017.12.045.

[23] O. Irulegi, L. Torres, A. Serra, I. Mendizabal, and R. Hernández, "The Ekihouse: An energy self-sufficient house based on passive design strategies," *Energy and Buildings,* vol. 83, pp. 57-69, 11// 2014, doi: http://dx.doi.org/10.1016/j.enbuild.2014.03.077.
[24] N. İ. Şahin and G. Manioğlu, "Water conservation through rainwater harvesting using different building forms in different climatic regions," *Sustainable Cities and Society,* vol. 44, pp. 367-377, 2019/01/01/ 2019, doi: https://doi.org/10.1016/j.scs.2018.10.010.
[25] V. Meera and M. M. Ahammed, "Water quality of rooftop rainwater harvesting systems: a review," *Journal of Water Supply: Research and Technology-AQUA,* vol. 55, no. 4, pp. 257-268, 2006.
[26] M. Z. I. Bashar, M. R. Karim, and M. A. Imteaz, "Reliability and economic analysis of urban rainwater harvesting: A comparative study within six major cities of Bangladesh," *Resources, Conservation and Recycling,* vol. 133, pp. 146-154, 2018, doi: 10.1016/j.resconrec.2018.01.025.
[27] Y. Tu, R. Wang, Y. Zhang, and J. Wang, "Progress and Expectation of Atmospheric Water Harvesting," *Joule,* vol. 2, no. 8, pp. 1452-1475, 2018/08/15/ 2018, doi: https://doi.org/10.1016/j.joule.2018.07.015.
[28] A. Entezari *et al.*, "Sustainable agriculture for water-stressed regions by air-water-energy management," *Energy,* vol. 181, pp. 1121-1128, 2019/08/15/ 2019, doi: https://doi.org/10.1016/j.energy.2019.06.045.
[29] M. Bohm, "Energy technology and lifestyle: A case study of the University at Buffalo 2015 Solar Decathlon home," *Renewable Energy,* vol. 123, pp. 92-103, 2018/08/01/ 2018, doi: https://doi.org/10.1016/j.renene.2018.02.029.
[30] C. Cornaro, S. Rossi, S. Cordiner, V. Mulone, L. Ramazzotti, and Z. Rinaldi, "Energy performance analysis of STILE house at the Solar Decathlon 2015: Lessons learned," *Journal of Building Engineering,* vol. 13, pp. 11-27, 2017/09/01/ 2017, doi: https://doi.org/10.1016/j.jobe.2017.06.015.
[31] S. Wang, F. Shi, B. Zhang, and J. Zheng, "The passive design strategies and energy performance of a zero-energy solar house: Sunny inside in solar decathlon China 2013," *Journal of Asian Architecture and Building Engineering,* Article vol. 15, no. 3, pp. 543-548, 2016, doi: 10.3130/jaabe.15.543.
[32] J. Vijayalaxmi, "Towards sustainable architecture – a case with Greentainer," *Local Environment,* vol. 15, no. 3, pp. 245-259, 2010/03/01 2010, doi: 10.1080/13549830903575596.
[33] H. Taleb, M. Elsebaei, and M. El-Attar, "Enhancing the sustainability of shipping container homes in a hot arid region: A case study of Aswan in Egypt," *Architectural Engineering and Design Management,* vol. 15, no. 6, pp. 459-474, 2019/11/02 2019, doi: 10.1080/17452007.2019.1628002.
[34] J. W. Axley and J. W. Axley, *Application of Natural Ventilation for US Commercial Buildings-Climate Suitability Design Strategies & Methods Modeling Studies*. US Department of Commerce, National Institute of Standards and Technology, 2001.
[35] M. Haase and A. Amato, "An investigation of the potential for natural ventilation and building orientation to achieve thermal comfort in warm and humid climates," *Solar energy,* vol. 83, no. 3, pp. 389-399, 2009.
[36] G. M. Elrayies, "Thermal Performance Assessment of Shipping Container Architecture in Hot and Humid Climates," *International Journal on Advanced Science, Engineering and Information Technology,* vol. 7, no. 4, pp. 1114-1126, 2017.
[37] H. Islam, G. Zhang, S. Setunge, and M. A. Bhuiyan, "Life cycle assessment of shipping container home: A sustainable construction," *Energy and Buildings,* vol. 128, pp. 673-685, 2016/09/15/ 2016, doi: https://doi.org/10.1016/j.enbuild.2016.07.002.

[38] A. M. Tanyer, A. Tavukcuoglu, and M. Bekboliev, "Assessing the airtightness performance of container houses in relation to its effect on energy efficiency," *Building and Environment,* vol. 134, pp. 59-73, 2018.
[39] T. Woods. "5 Methods to Insulate Your Shipping Container Home." http://www.containerhomeplans.org/2015/03/5-methods-to-insulate-your-shipping-container-home/ (accessed.
[40] S. Geving, "Smarte dampsperrer – et spennende nytt alternativ!," ed, 2012.
[41] A. Dalehaug, "Email correspondace 16.05," ed, 2017.
[42] S. Wu, X. Zheng, C. You, and C. Wei, "Household energy consumption in rural China: Historical development, present pattern and policy implication," *Journal of cleaner production,* vol. 211, pp. 981-991, 2019.
[43] B.-J. He, L. Yang, and M. Ye, "Building energy efficiency in China rural areas: Situation, drawbacks, challenges, corresponding measures and policies," *Sustainable Cities and Society,* vol. 11, pp. 7-15, 2014.
[44] M. Evans, S. Yu, B. Song, Q. Deng, J. Liu, and A. Delgado, "Building energy efficiency in rural China," *Energy Policy,* vol. 64, pp. 243-251, 2014.
[45] X. Juan and G. Weijun, "Analysis on energy consumption of rural building based on survey in northern China," *Energy for sustainable development,* vol. 47, pp. 34-38, 2018.
[46] M. Shan, P. Wang, J. Li, G. Yue, and X. Yang, "Energy and environment in Chinese rural buildings: Situations, challenges, and intervention strategies," *Building and Environment,* vol. 91, pp. 271-282, 2015.
[47] Q. Li *et al.,* "Impacts of household coal and biomass combustion on indoor and ambient air quality in China: Current status and implication," *Science of The Total Environment,* vol. 576, pp. 347-361, 2017/01/15/ 2017, doi: https://doi.org/10.1016/j.scitotenv.2016.10.080.
[48] F. Wang, H. Wang, and Y. Wang, "Tests Analysis of Heating Energy Consumption and Indoor Air Quality in Northeastern Rural Dwellings of China," *Procedia Engineering,* vol. 146, pp. 17-23, 2016/01/01/ 2016, doi: https://doi.org/10.1016/j.proeng.2016.06.347.
[49] B. P. Jelle, "Traditional, state-of-the-art and future thermal building insulation materials and solutions – Properties, requirements and possibilities," *Energy and Buildings,* vol. 43, no. 10, pp. 2549-2563, 10// 2011, doi: http://dx.doi.org/10.1016/j.enbuild.2011.05.015.
[50] EQUA. "IDA Indoor Climate and Energy." https://www.equa.se/en/ida-ice (accessed.
[51] EQUA. "IDA Indoor Climate and Energy." http://www.equa.se/en/ida-ice (accessed.
[52] Y. Goto, Y. Ostermeyer, and H. Wallbaum, "Transfer of energy efficient building concepts to subtropical climate–The first MINERGIE P® based building in Japan," in *10th Nordic Symposium on Building Physics, 15-19 June 2014, Lund,* 2014.
[53] Separett. "Separett Villa." https://www.separett-usa.com/index.php/waterless-urine-diverting-toilet.html (accessed.
[54] G. Morrison. "Composting Toilet Options For Tiny Houses." https://tinyhousebuild.com/composting-toilet-options/ (accessed.
[55] B. Cao, Y. Tu, and R. Wang, "A Moisture-Penetrating Humidity Pump Directly Powered by One-Sun Illumination," *iScience,* vol. 15, pp. 502-513, 2019.
[56] Panasonic. "Vacuum Insulation: Vacuum Insulation Panel (VIP)." https://eu.industrial.panasonic.com/products/motors-compressors-pumps/vacuum-insulation/vacuum-insulation-panel-vip (accessed.
[57] *ISO 9869-1:2014 Thermal insulation — Building elements — In-situ measurement of thermal resistance and thermal transmittance — Part 1: Heat flow meter method,* ISO, 2014. [Online]. Available: https://www.iso.org/standard/59697.html

[58] PHI, "Criteria for the Passive House, EnerPHit and PHI Low Energy Building Standard," 2016. [Online]. Available: https://passiv.de/downloads/03_building_criteria_en.pdf
[59] *DGJ 08-205-2015 Design standard for energy efficiency of residential buildings*, S. Construction, 2016.
[60] *EN 16798-1:2019 Energy performance of buildings - Ventilation for buildings - Part 1*, CEN, 2019. [Online]. Available: https://www.standard.no/no/Nettbutikk/produktkatalogen/Produktpresentasjon/?ProductID=1055687
[61] P. Heiselberg, K. Svidt, and P. V. Nielsen, "Characteristics of airflow from open windows," *Building and Environment*, vol. 36, no. 7, pp. 859-869, 2001.
[62] *GB/T18883-2002 China Indoor Air Quality Standard*, Beijing, 2002.
[63] A. Persily and L. de Jonge, "Carbon dioxide generation rates for building occupants," *Indoor air*, vol. 27, no. 5, pp. 868-879, 2017.
[64] M. W. Liddament, *Air infiltration calculation techniques: An applications guide*. AIVC, Bracknell, 1999.
[65] H. Energy. "Homer Pro." https://www.homerenergy.com/products/pro/index.html (accessed.
[66] J.-H. Kim, F. E. Boafo, S.-M. Kim, and J.-T. Kim, "Aging performance evaluation of vacuum insulation panel (VIP)," *Case Studies in Construction Materials*, vol. 7, pp. 329-335, 2017/12/01/ 2017, doi: https://doi.org/10.1016/j.cscm.2017.09.003.
[67] Y. Zhou and R. S. Tol, "Water use in China's domestic, industrial and agricultural sectors: An empirical analysis," *FNU-67*, pp. 85-93, 2005.
[68] C. M. Silva, V. Sousa, and N. V. Carvalho, "Evaluation of rainwater harvesting in Portugal: Application to single-family residences," *Resources, Conservation and Recycling*, vol. 94, pp. 21-34, 1// 2015, doi: https://doi.org/10.1016/j.resconrec.2014.11.004.
[69] S. Zhang, J. Zhang, T. Yue, and X. Jing, "Impacts of climate change on urban rainwater harvesting systems," *Science of The Total Environment*, vol. 665, pp. 262-274, 2019/05/15/ 2019, doi: https://doi.org/10.1016/j.scitotenv.2019.02.135.
[70] H. E. Beck, N. E. Zimmermann, T. R. McVicar, N. Vergopolan, A. Berg, and E. F. Wood, "Present and future Köppen-Geiger climate classification maps at 1-km resolution," *Scientific Data*, Data Descriptor vol. 5, p. 180214, 10/30/online 2018, doi: 10.1038/sdata.2018.214.
[71] C. Dara and C. Hachem-Vermette, "Evaluation of low-impact modular housing using energy optimization and life cycle analysis," *Energy, Ecology and Environment*, journal article vol. 4, no. 6, pp. 286-299, December 01 2019, doi: 10.1007/s40974-019-00135-4.